Inorg. Chem. **2008**, *47*, 1460−1464

Unique Manganese Phosphorus Complex with a Mn_5P_7 Core: Synthesis, Molecular Structure, and Magnetic Properties

Carsten von Hänisch,*,† Florian Weigend,*,† and Rodolphe Clérac‡

Institut für Nanotechnologie, Forschungszentrum Karlsruhe GmbH, P.O. Box 3640, D-76021 Karlsruhe, Germany, and Université Bordeaux 1, CNRS, Centre de Recherche Paul Pascal−UPR8641, 115 Avenue du Dr. Albert Schweitzer, 33600 Pessac, France

Received August 29, 2007

The manganese phosphorus cluster $[Mn_5\{N(SiMe_3)_2\}\{\mu_4\text{-}PSi\textit{i}Pr_3\}_2\{\mu\text{-}P(H)Si\textit{i}Pr_3\}_5]$ (**1**) containing an unusual Mn_5P_7 core structure and three short Mn−Mn distances was obtained from the reaction of $Mn\{N(SiMe_3)_2\}_2$ with $H_2PSi\textit{i}Pr_3$. Quantum chemical investigations indicated the presence of comparably strong intramolecular antiferromagnetic interactions leading to a total $S = 5/2$ spin ground state, which was confirmed by magnetic measurements.

Introduction

For the last two decades, various polynuclear manganese complexes and clusters have been synthesized.[1] They are of considerable interest because of their magnetic properties and possible applications as single molecule magnets (SMMs). In these compounds, the Mn atoms usually are bridged by ligands with light donor atoms such as oxo, alkoxy, or carboxyl groups. For this type of bridging, in most cases, Mn(II) centers are antiferromagnetically coupled, and wavenumbers for coupling parameters typically are in the range of a few cm^{-1}.[2] Clusters with bridging ligands containing heavier donor atoms[3] in contrast, are much rarer; the only phosphorus bridged Mn clusters presently known to us are the carbonyl compounds $[Mn(CO)_4(\mu\text{-}PH_2)]_n$ ($n = 2, 3$) and $[Mn_2(CO)_6(\mu\text{-}CO)(\mu\text{-}PPh_2)_2]$ as well as some mixed metal species such as $[\{Mn(CO)_4\}_2(AuPPh_3)(\mu\text{-}H)(\mu_3\text{-}PCy)]$ (Cy = cyclohexyl).[4] One might expect that magnetic coupling via ligands with P atoms will lead to coupling parameters significantly different from those containing O or N atoms because of differences in energy and expansiveness of the p-orbitals as well as in the electronegativity of the respective elements.

The compound presented here is uncommon for a further reason. Indeed, primary silyl phosphines (R_3SiPH_2) are frequently used for the synthesis of phosphorus bridged multinuclear complexes, but these complexes typically contain main group metals; they exhibit a structural variety including cages, heteroatom centered clusters, as well as mixed valent compounds.[5] In comparison, much less is known about corresponding transition metal species.[6]

* To whom correspondence should be addressed. E-mail: florian.weigend@int.fzk.de, carsten.vonhaenisch@int.fzk.de; fax: +49 (0)7247 82-6368.

† Institut für Nanotechnologie.

‡ Université Bordeaux 1, CNRS, CRPP.

(1) (a) Ako, A. M.; Hewitt, I. J.; Mereacre, V.; Clŕac, R.; Wernsdorfer, W.; Anson, C. E.; Powell, A. K. *Angew. Chem.* **2006**, *118*, 5048–5051 ; *Angew. Chem., Int. Ed.* **2006**, *45*, 4926–4929. (b) Stamatatos, T. C.; Abboud, K. A.; Wernsdorfer, W.; Christou, G. *Angew. Chem.* **2006**, *118*, 4240–4243 ; *Angew. Chem., Int. Ed.* **2006**, *45*, 41342–4137. (c) Christou, G. *Polyhedron* **2005**, *24*, 2065–2075. (d) Christou, G.; Gatteschi, D.; Hendrickson, D. N.; Sessoli, R. *MRS Bull.* **2000**, *25*, 66–71.

(2) (a) For further examples, see also references within: Gultneh, Y.; Tesema; Y. T.; Ahvazi, B.; Yisgedu, T. B.; Butcher; R. J.; Tuchagues, J.-P. *Inorg. Chim. Acta* **2006**, *359*, 4463–4469. (b) Karmakar, T. K.; Ghosh, B. K.; Usman, A.; Fun, H.-K.; Rivière, E.; Mallah, T.; Aromi, G.; Chandra, S. *Inorg. Chem.* **2005**, *44*, 2391–2399. (c) Humphrey, S. M.; Mole, R. A.; Rawson, J. M.; Wood, P. *Dalton Trans.* **2004**, 1670–1678. (d) Ryazanov, M.; Troyanov, S.; Baran, M.; Szymczak, R.; Kuzmina, N. *Polyhedron* **2004**, *23*, 879–883. (e) Martin, J. D.; Hess, R. F.; Boyle, P. D. *Inorg. Chem.* **2004**, *43*, 3242–3247.

(3) (a) Melullis, M.; Clérac, R.; Dehnen, S. *Chem. Commun.* **2005**, 6008–6010. (b) Brandmayer, M. K.; Clŕac, R.; Weigend, F.; Dehnen, S. *Chem.—Eur. J.* **2004**, *10*, 5147–5157. (c) Shieh, M.; Chen, H.-S.; Yang, H.-Y.; Lin, S.-F.; Ueng, C.-H. *Chem.—Eur. J.* **2001**, *7*, 3152–3158. (d) Shieh, M.; Chen, H.-S.; Yang, H.-Y.; Ueng, C.-H. *Angew. Chem.* **1999**, *111*, 1339–1341 ; *Angew. Chem., Int. Ed.* **1999**, *38*, 1252–1254. (e) Seidel, R.; Schnautz, B.; Henkel, G. *Angew. Chem.* **1996**, *108*, 1836–1839 ; *Angew. Chem., Int. Ed.* **1996**, *35*, 1710–1712. (f) Haupt, H.-J.; Schwefer, M.; Egold, H.; Flŕke, U. *Inorg. Chem.* **1995**, *34*, 5461–5467.

(4) (a) Haupt, H.-J.; Schwefer, M.; Egold, H.; Flörke, U. *Inorg. Chem.* **1995**, *34*, 5461–5467. (b) Deppisch, B.; Schäfer, H.; Binder, D.; Leske, W. *Z. Anorg. Allg. Chem.* **1984**, *519*, 53–66. (c) Kawamura, T.; Sowa, T.; Yonezawa, T.; Yamabe, T.; Masuda, H.; Taga, T.; Machida, K. *J. Organomet. Chem.* **1984**, *276*, 10–12.

(5) (a) Neumüller, B.; Iravani, E. *Coord. Chem. Rev.* **2004**, *248*, 817–834. (b) Driess, M.; Mulvey, R. E.; Westerhausen, M. In *Molecular Clusters of the Main Group Elements*; Driess, M., Nöth, H., Eds.; Wiley-VCH: Weinheim, Germany, 2004; pp 391–424.

10.1021/ic701694f CCC: $40.75
Published on Web 02/01/2008

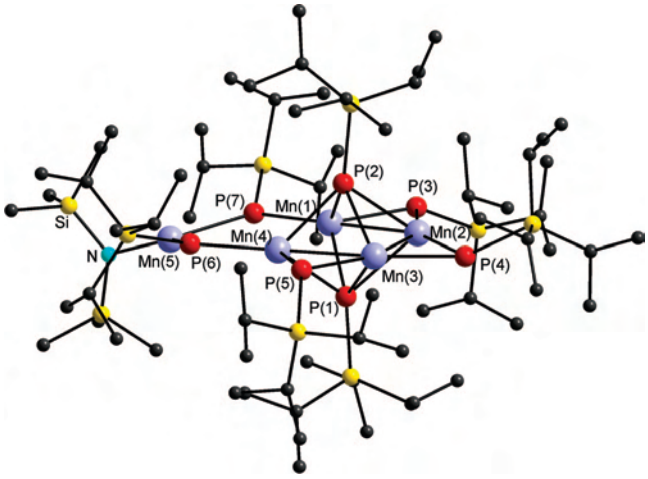

Figure 1. Molecular structure of **1**. Hydrogen atoms are omitted for clarity. Selected bond length (pm) and bond angles (deg): Mn(1)−Mn(2) 274.74(13), Mn(2)−Mn(3) 267.51(12), Mn(3)−Mn(4) 276.27(13), P−Mn 242.95(14)−257.65(16), P−Si 223.9(2)−227.1(2), N−Mn(5) 199.2(4), and N−Si 170.0(5) and 170.2(5); Mn(1)−Mn(2)−Mn(3) 95.09(4), Mn(2)−Mn-(3)−Mn(3) 95.20(4), and P(6)−Mn(5)−P(7) 99.75(6).

In the course of our studies, we investigated reactions of the amide $Mn\{N(SiMe_3)_2\}_2$ with primary silylphosphines to obtain phosphorus bridged manganese compounds. In the following, we describe the synthesis and the structural characterization of the exclusively phosphorus bridged manganese cluster $[Mn_5\{N(SiMe_3)_2\}\{\mu_4\text{-}PSi\textit{i}Pr_3\}_2\{\mu\text{-}P(H)\text{-}Si\textit{i}Pr_3\}_5]$ (**1**) obtained from the reaction of $Mn\{N(SiMe_3)_2\}_2$ with $H_2PSi\textit{i}Pr_3$. Magnetic coupling parameters were calculated within a Heisenberg model by means of a broken-symmetry treatment using hybrid density functional methods; the temperature dependency of the magnetic susceptibility modeled with this set of parameters was compared to experimental data.

Results and Discussion

Structural Characterization. Compound **1** crystallized from the reaction mixture at −30 °C in the triclinic space group $P\bar{1}$ ($\mathbf{1}\cdot 1/2Et_2O$ ($C_{69}H_{170}NMn_5P_7Si_9\cdot 1/2C_4H_{10}O$, M = 1795.46); a = 1456.7(3) pm, b = 1712.1(3) pm, c = 2124.8(4) pm, $\alpha = 96.01(3)°$, $\beta = 91.81(3)°$, $\gamma = 99.59(3)°$).

As shown in Figure 1, the molecular structure consists of five manganese atoms, five μ_2-P(H)Si*i*Pr$_3$ groups, two μ_4-PSi*i*Pr$_3$ groups and one exocyclic $N(SiMe_3)_2$ ligand. The Mn atoms Mn(1)−Mn(4) form a trapezium with a comparably long edge Mn(1)−Mn(4) 317.0 pm, and three edges (bridged by μ_2-P(H)Si*i*Pr$_3$ groups) with distances of 274.7 pm for Mn(1)−Mn(2), 276.3 pm for Mn(3)−Mn(4), and 267.5 pm for Mn(2)−Mn(3); this is less than is usually observed for Mn−Mn single-bond distances (278–293 pm).[3,4,7] Two additional μ_4-PSi*i*Pr$_3$ ligands are located above and below the Mn_4 fragment. By two further μ_2-P(H)Si*i*Pr$_3$ units, Mn(1) and Mn(4) are connected to the fifth manganese atom, Mn(5). This atom bonds to a terminal $N(SiMe_3)_2$ ligand. Each of the manganese atoms Mn(1)−Mn(4) are (distorted) tetrahedrally surrounded by four phosphorus atoms. These tetrahedrals are face-linked along the Mn(1)−Mn(2), Mn(2)−Mn-(3), and Mn(3)−Mn(4) axes, whereas the tetrahedrals surrounding Mn(1) and Mn(4) are edge-linked. The Mn−P bonds lengths in **1** range from 243 to 257 pm and are therefore larger than in other phosphorus bridged manganese compounds (e.g., 235.0–238.9 pm for the cyclic compound $[Mn(CO)_4(\mu_2\text{-}PH_2)]_n$ (n = 2, 3)).[4]

The phosphorus-bound hydrogen atoms of the P(H)Si*i*Pr$_3$ (P(3)−P(7)) groups could not be located in the difference Fourier analysis of the X-ray data; however, the presence of the H atoms is chemically plausible, as in this case Mn centers were doubly oxidized throughout. The IR spectrum of **1** shows a strong peak at 2298 cm^{-1} that is assigned to the P−H stretching vibration. Other metal derivatives of primary silyl phosphines show very similar values. Example are $[(DME)LiP(H)Si\textit{t}Bu_3]_2$ (2261 cm^{-1}), $[Et_2InP(H)Si\textit{i}Pr_3]_2$ (2308 cm^{-1}), or $[O\{Si\textit{i}Pr_2P(H)AlEt_2\}_2]_4$ (2300 cm^{-1}).[8]

Quantum Chemical Investigations. Quantum chemical calculations were carried out to give insight as to the magnetic properties of compound **1** by considering high-spin and broken-symmetry states.[9,10] Methods of density functional theory, as implemented in the program system TURBOMOLE,[11–13] were used in connection with the basis sets of type def2-TZVP[14] plus corresponding Coulomb fitting basis sets.[14] The B3-LYP functional[15] was chosen, as it yields comparably reliable values for spin–spin coupling parameters.[10]

The presence of five Mn(II) centers leads to a total spin of 25/2 in the case of parallel spins for all Mn atoms; furthermore, one might consider altogether 15 states with opposite spin orientations for different Mn atoms, the so-called broken-symmetry states. The latter are no pure spin states but mixtures of them. Nevertheless, from the energy differences of the broken-symmetry states to the high-spin state, E_{rel}, the estimation of spin–spin coupling parameters within a phenomenological Heisenberg model is possible.[9,10]

At first, the high-spin state was treated; here and as long as not mentioned otherwise, structure parameters were taken from the X-ray data. The converged wave function shows an energetic gap between occupied and virtual orbitals of

(6) (a) Wiberg, N.; Wörner, A.; Fenske, D.; Nöth, H.; Knizek, J.; Polborn, K. *Angew. Chem.* **2000**, *112*, 1908–1912 ; *Angew. Chem., Int. Ed.* **2000**, *39*, 1838–1842. (b) Driess, M.; Martin, S.; Merz, K.; Pintchouk, V.; Pritzkow, H.; Grützmacher, H.; Kaupp, M. *Angew. Chem.* **1997**, *109*, 1982–1985 ; *Angew. Chem., Int. Ed.* **1997**, *36*, 1894–1897.
(7) Bianchi, R.; Gervasio, G.; Marabello, D. *Inorg. Chem.* **2000**, *39*, 2360–2366.
(8) (a) von Hänisch, C.; Stahl, S. *Angew. Chem.* **2006**, *118*, 2360–2363 ; *Angew. Chem., Int. Ed.* **2006**, *45*, 2302–2305. (b) Westerhausen, M.; Weinrich, S.; Schmid, B.; Schneiderbauer, S.; Suter, M.; Nöth, H.; Piotrowski, H. *Z. Anorg. Allg. Chem.* **2003**, *629*, 625–633. (c) von Hänisch, C.; Rolli, B. *Z. Anorg. Allg. Chem.* **2002**, *628*, 2255–2258.
(9) Noodleman, L.; Case, D.; Aizman, A. *J. Am. Chem. Soc.* **1988**, *110*, 1001–1005.
(10) Ruiz, E.; Cano, J.; Alvarez, S.; Alemany, P. *J. Comput. Chem.* **1999**, *20*, 1391–1400.
(11) *TURBOMOLE*, version 5.9; Universität Karlsruhe: Karlsruhe, Germany, 2006.
(12) Treutler, O.; Ahlrichs, R. *J. Chem. Phys.* **1995**, *102*, 346–354.
(13) Eichkorn, K.; Treutler, O.; Oehm, H.; Häser, M.; Ahlrichs, R. *Chem. Phys. Lett.* **1995**, *240*, 283–290.
(14) (a) Weigend, F.; Ahlrichs, R. *Phys. Chem. Chem. Phys.* **2005**, *7*, 3297–3305. (b) Weigend, F. *Phys. Chem. Chem. Phys.* **2006**, *8*, 1057–1065.
(15) Lee, C.; Yang, W.; Parr, R. G. *Phys. Rev. B: Condens. Matter Mater. Phys.* **1988**, *37*, 785–789.

Table 1. Relative Energies of Broken-Symmetry States with Respect to High-Spin State, E_{rel}

E_{rel} (kJ mol^{-1})			
$S = 15/2$		$S = 5/2$	
uduuu	−81.2	*ududu*	−123.5
uuduu	−79.5	*duduu*	−123.4
duuuu	−58.2	*duudu*	−85.3
uuudu	−56.5	*uduud*	−85.9
uuuud	−5.4	*uudud*	−84.1
		uddduu	−81.7
		uuddu	−69.9
		dduuu	−69.8
		duuud	−58.4
		uuudd	−56.6

2.0 eV, the numbers of unpaired d-electrons per Mn atom (calculated via Mulliken population analysis) are 4.8–4.9, close to the expected value for Mn(II), 5.0. Next, all broken-symmetry states were treated (i.e., five states with $S = 15/2$ and 10 states with $S = 5/2$, specified on the left-hand side of Table 1); as an example, *ududu* means a surplus of five spin-up electrons for Mn(1), Mn(3), and Mn(5) (see also Figure 1) and a surplus of (approximately) five spin-down electrons for Mn(2) and Mn(4). Start orbitals were generated from state *uuuuu* by first applying a Boys and Foster localization procedure[16] on the valence (spin) orbitals and then flipping the spin for the five localized d-orbitals at the desired atoms. The facility of breaking spin symmetry in this easily operated way was implemented in TURBOMOLE in this context. SCF procedures lead to single-point energies for the 15 broken-symmetry states. The resulting energy differences toward the high-spin state are listed on the left-hand side of Table 1. Mulliken population analyses show absolute values of 4.6–4.9 unpaired d-electrons for all Mn atoms for all cases.

The two states with alternating surpluses of spin-up and spin-down electrons in the Mn(1)−Mn(2)−Mn(3)−Mn(4) quadrangle, *ududu* and *duduu*, are by far the lowest in energy, $E_{rel} = -123$ kJ/mol. The other broken-symmetry states show relative energies of −55 to −85 kJ/mol, except for *uuuud*, which is nearly as unfavorable as the high-spin state, $E_{rel} = -5$ kJ/mol. Moreover, the approximate C_s symmetry of the molecule is reflected in E_{rel}. States being symmetry-equivalent in C_s differ by less than 2 kJ/mol at the most.

To determine spin–spin coupling constants within a Heisenberg model[10,17] with the phenomenological Hamiltonian

$$\hat{H} = -\sum_{i>j} J(i,j)\hat{S}_i\hat{S}_j \qquad (1)$$

the relative energies E_{rel} are decomposed into a sum of energies $e(i,j)$ due to interactions of opposite spins at Mn(i)−Mn(j) atom pairs. For *ududu*, for example, E_{rel} may be decomposed into the sum of energy gains $e(1,2) + e(2,3) + e(3,4) + e(4,1) + e(5,1) + e(5,3)$. The resulting overdetermined system of equations (15 broken-symmetry states vs 10 different pairs of energies to be evaluated) was solved by minimizing the quadratic deviation to E_{rel} for the whole ensemble. From the $e(i,j)$, the $J(i,j)$ coupling constants can be determined[16]

$$J(i,j) = \frac{e(i,j)}{2S(i)S(j) + S(j)} \qquad (2)$$

Coupling constants obtained this way for $S(i) = S(j) = 5/2$ are listed in Table 2. All coupling constants are of negative sign and decrease for increasing Mn−Mn distances d. The parameters listed in Table 2 were used for the simulation of the experimentally measured temperature dependence of the magnetic susceptibility, leading to reasonable agreement. They are significantly larger than values typically obtained for Mn(II) centers bridged by ligands containing atoms of the second period,[2] even if we have to admit that with the chosen method the coupling parameters are probably calculated somewhat too large. For a direct comparison of bridges consisting of second- and third-period elements, we calculated Mn_2L_2 cycles (L = NH, PH, $PSiMe_3$) and found the coupling parameters for PH and $PSiMe_3$ to be more than 3 times as large as that for NH.

Table 2. Parameters of Magnetic Coupling between Atoms Mn(i) and Mn(j) of **1**, $J(i,j)$, Resulting from a Heisenberg Model Using Relative Energies Listed in Table 1[a]

coupling constants	
i, j	J (cm^{-1})
3,2	−219.8
2,1	−192.3
4,3	−182.6
4,1	−79.1
3,1	−38.1
4,2	−38.1
5,4	−13.3
5,1	−12.7
5,3	−1.7
5,2	−1.6

[a] For details, see text.

Next, geometric structure parameters were optimized for all states being symmetry-distinct in C_s symmetry; moreover, now the Si*i*Pr$_3$ groups were replaced with $SiMe_3$. For the resulting nine broken-symmetry states, stabilities relative to the high-spin state and deviations of structure parameters from experimental data are listed in Table 3.

Calculated structure parameters are in reasonable agreement (ca. +3...+5 pm) with experimentally determined ones only for the state *duduu* (which in C_s symmetry is identical to *ududu*). The other states show large deviations (ca. +8...+25 pm) always for those distances, for which spins are parallel instead of antiparallel for neighboring Mn atoms. Relative energies show the same trend as stated previously: the relaxation of structure parameters for the energetically unfavorable states leads to somewhat smaller values for E_{rel}, but state *duduu* is still clearly favored.

The comparably large effects of spin orientations on structure parameters (shorter/longer distances for antiparallel/parallel spins) are in line with higher/lower electron densities along the Mn−Mn bonds between atoms of opposite/same spin. The difference of the total electron densities of the two states *uuuuu* and *duduu* is shown in Figure 2. For *uuuuu*,

(16) Foster, J. M.; Boys, S. F. *Rev. Mod. Phys.* **1960**, *32*, 300.
(17) Ruiz, E.; Rodriguez-Fortea, A.; Cano, J.; Alvarez, S.; Alemany, P. *J. Comput. Chem.* **2002**, *24*, 982–989.

Table 3. Data for Optimized Structures of States Being Symmetry-Distinct in C_s Symmetry[a]

		differences of calculated and experimental distances (pm)					
state	E_{rel} (kJ mol^{-1})	Mn(i)−Mn(j)				∅(Mn−P)	σ(Mn−P)
		1–2	2–3	3–4	4–1		
duduu	−90	+4.0	+5.5	+3.4	+5.6	+2.9	1.1
uudud	−61	+18.3	+5.7	+0.7	+14.7	+4.4	2.7
duudu	−50	+3.6	+17.8	+2.5	+14.0	+4.2	2.0
udduu	−47	+3.8	+17.9	+2.7	+13.2	+4.4	1.8
uuddu	−46	+17.5	+8.05	+15.9	−2.4	+4.9	2.0
uuudd	–42	+22.3	+22.9	+2.2	–3.1	+5.3	3.4
uuduu	–57	+18.5	+5.8	+0.9	+14.1	+4.6	2.7
uuudu	–43	+22.3	+23.0	+2.3	–3.5	+5.3	3.5
uuuud	–5	+19.3	+24.7	+18.3	+9.2	+7.4	3.0
uuuuu	0	+19.4	+24.7	+18.3	+8.0	+7.5	2.7

[a] E_{rel} denotes the relative energy as compared to the high-spin state; in the columns, differences of calculated and experimental distances are given. [∅(Mn–P) and σ(Mn–P) denote average error and standard deviation of errors for the 18 Mn–P bonds.

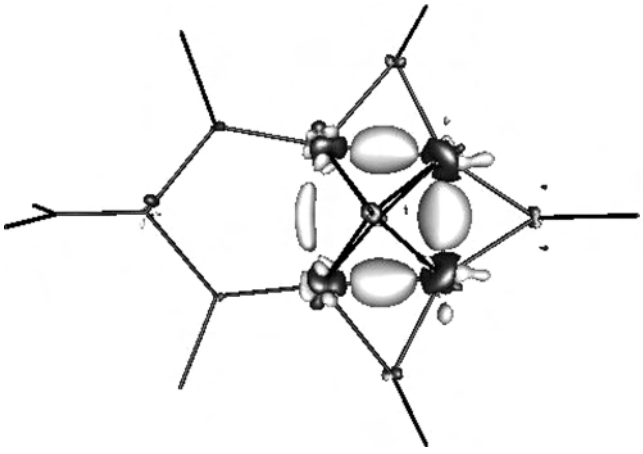

Figure 2. Difference of total electron densities of states *duduu* ($S = 5/2$) and *uuuuu* ($S = 25/2$). Dark color indicates larger electron density for *uuuuu*, and white represents *duduu*. Surfaces are drawn at values of $\pm 10^{-3}$ electrons/r_B^3 (r_B is the Bohr radius, 52.92 pm).

Pauli repulsion leads to a reduced electron density between the Mn atoms. For *duduu*, this repulsion is not present between neighboring Mn atoms allowing for a (small) delocalization of the d-orbitals along these axes.

Investigation of the spin density (i.e., the difference between electron densities of spin-up and spin-down electrons) indicates that the spins at the neighboring Mn atoms are coupled by superexchange via the bridging P atoms. In Figure 3, the spin density is shown for the state *duduu*. Besides the alternating surplus of spin-up and spin-down electrons for neighboring Mn atoms (except for Mn(4)−Mn(5)), the opposite spin-polarization of the p-orbitals of the bridging P atoms in the molecular plane also is visible.

Magnetic Measurements. Magnetic measurements have been performed on a polycrystalline sample of **1** (see Figure 4). Decreasing the temperature, the χT product continuously decreases from 5.3 cm^3 K/mol at room temperature to reach a constant value of 4.3 cm^3 K/mol below 20 K. This indicates dominant antiferromagnetic interactions in the Mn_5 complex already suggested by the DFT analysis. It is worth noting that our attempts failed to model the magnetic susceptibility directly with a five $S = 5/2$ classical spin Heisenberg model.

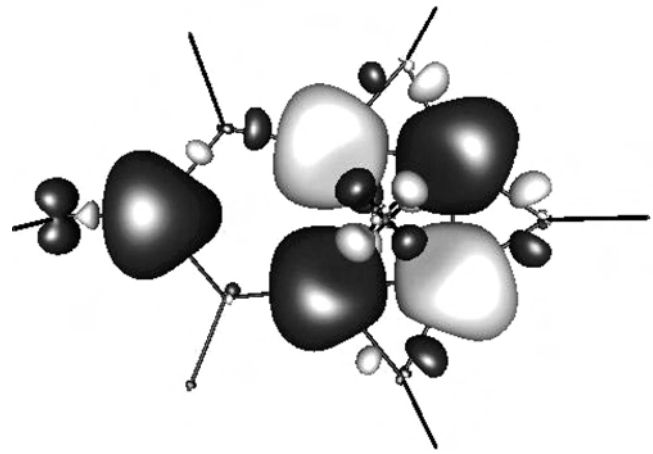

Figure 3. Difference of spin-up and spin-down electron densities for state *duduu* ($S = 5/2$). Dark color indicates a surplus of spin-up, and light color represents a surplus of spin-down electrons. Surfaces are drawn at values of $\pm 3 \times 10^{-3}$ electrons/r_B^3.

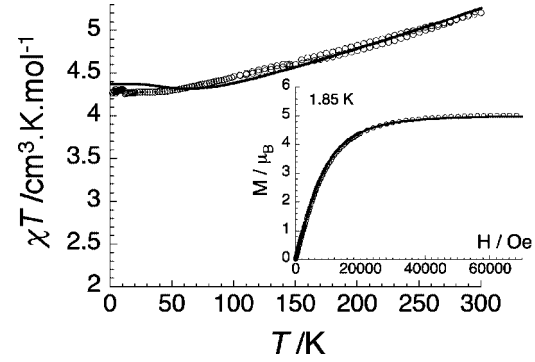

Figure 4. Temperature dependence of the χT product (where $\chi = M/H$) of **1** measured in $H_{dc} = 1000$ Oe. The solid line is the calculated susceptibility[18] obtained from the interaction parameters estimated by DFT calculations. Inset: field dependence of the magnetization at 1.85 K. The solid line is the best fit obtained with an $S = 5/2$ Brillouin function and $g = 1.99$.

Indeed, the simulation was not possible even with a simplified (i.e., symmetrized) cluster taking into account only three magnetic interactions. Unfortunately, when four or more couplings were considered, the resulting parameters were physically meaningless with error values of the order of the value itself (i.e., leading to overparametrization). Therefore, the DFT approach has been the only way to evaluate the exchange parameters in this system and to compare with experiment. As shown in Figure 4, the calculated temperature dependence of the magnetic susceptibility[18] obtained considering the DFT interaction parameters (vide supra) is in reasonable agreement with the experimental data. Below 20 K, the value of the χT product indicates an $S = 5/2$ spin ground-state with a g factor of 1.98 ($S = 5/2$ Mn(II) metal ions: $C = 4.375$ cm^3 K/mol with $g = 2$). In addition, the field dependence of magnetization at 1.85 K (inset of Figure 4) can be fitted remarkably well to an $S = 5/2$ Brillouin function with $g = 1.99$ that confirms the $S = 5/2$ ground-state of this complex.

(18) (a) Borrás-Almenar, J. J.; Clemente-Juan, J. M.; Coronado, E.; Tsukerblat, B. S. *Inorg. Chem.* **1999**, *38*, 6081. (b) Borrás-Almenar, J. J.; Clemente-Juan, J. M.; Coronado, E.; Tsukerblat, B. S. *J. Comput. Chem.* **2001**, *22*, 985.

In conclusion, the quantum chemical results of compound **1** confirm the presence of five Mn(II) atoms. Moreover, they agree with the alternated spin orientation suggested by the magnetic measurements that leads to a total spin ground-state of $S = 5/2$.

Experimental Procedures

All manipulations were carried out under rigorous exclusion of oxygen and moisture, using a Schlenk line and nitrogen atmosphere. Solvents were dried and freshly distilled before use. The starting materials were prepared in the manner described in the literature.[19] The magnetic susceptibility measurements were obtained with the use of a Quantum Design SQUID magnetometer MPMS-XL. This magnetometer works between 1.8 and 400 K for dc applied fields ranging from –7 to 7 T. Measurements were performed on a polycrystalline sample of 23.0 mg. The absence of ferromagnetic impurities was checked by measuring the magnetization as a function of the dc field at 100 K. The magnetic data were corrected for the sample holder and the diamagnetic contribution.

1: 0.20 mL (0.88 mmol) of $H_2PSi\textit{i}Pr_3$ was added to a solution of 0.33 g (0.88 mmol) of $Mn\{N(SiMe_3)_2\}_2$ in 10 mL of ether at −60 °C. The reaction mixture was warmed to room temperature and stirred for 16 h. After reduction of the volume to 5 mL, the red solution was cooled to −35 °C. Red crystals of **1**·1/2Et_2O appeared within 3 days. Yield: 0.20 g (88% based on phosphorus). Elemental analysis (%): calcd for $C_{69}H_{170}NMn_5P_7Si_9$·1/2$C_4H_{10}O$ (1795.46): C 47.50, H 9.82, N 0.78; found: C 47.65, H 10.18, N 0.68.

IR (KBr) (cm^{-1}): 2942 (s), 2928 (vs), 2863 (vs), 2298 (s), 1958 (w), 1462 (vs), 1383 (s), 1364 (s), 1289 (m), 1244 (s), 1180 (w), 1157 (w), 1070 (s), 1017 (s), 994 (vs), 918 (s), 880 (vs), 841 (s), 824 (s), 781 (m), 749 (m), 661 (vs), 639 (vs), 572 (vs), 538 (w), 511 (vs), 478 (s), 430 (m), 405 (w).

Supporting Information Available: X-ray crystallographic file in CIF format. This material is available free of charge via the Internet at http://pubs.acs.org.

IC701694F

(19) (a) Westerhausen, M.; Löw, R.; Schwarz, W. *J. Organomet. Chem.* **1996**, *513*, 213–229. (b) Bürger, H.; Wannagat, U. *Mh. Chem.* **1964**, *95*, 1099–1102.